Eur Biophys J (1997) 26: 183–193

ARTICLE

W. Wiczk · L. Łankiewicz · F. Kasprzykowski
S. Ołdziej · H. Szmaciński · J. R. Lakowicz · Z. Grzonka

Fluorescence study of neurohypophyseal hormones and their analogues

Distance distributions in a series of arginine-vasopressin analogues

Received: 5 August 1996 / Accepted: 8 December 1996

Abstract Analogues of arginine-vasopressin (AVP) in which substitution of the proline residue in position 7 (by either sarcosine or N-methylalanine) combined with replacement of the cysteine residue in position 1 were the subject of a fluorescence and molecular mechanics study. We obtained two groups of analogues: selective antidiuretic agonists (cysteine or β-mercaptopropionic acid in position 1) and pressor and uterotonic antagonists (deaminopenicillamine or β-mercapto-β,β-cyclopentamethylenepropionic acid in position 1). Using frequency-domain measurements of fluorescence resonance energy transfer (FRET) we estimated the distance distribution between the phenolic ring of Tyr^2 and the disulphide bridge Cys^1–Cys^6. We also analyzed acrylamide quenching of tyrosyl fluorescence to determine the exposure of the tyrosyl ring to the solvent. Results from fluorescence experiments were compared with those from Monte Carlo simulation (ECEPP/3 force-field).

Key words Arginine-vasopressin analogues · Energy transfer · Fluorescence quenching · Acrylamide · Molecular mechanics

Abbreviations AVP Arginine-vasopressin · Sar Sarcosine · MeAla N-methyl-alanine · Mpa β-mercaptopropionic acid · Dmp β-mercapto-β,β-dimethylpropionic acid (deaminopenicillamine) · Cpp β-mercapto-β,β-cyclopentamethylenepropionic acid · Asu Aminosuberic acid · EDMC Electrostatically-Driven Monte Carlo · ECEPP Empirical Conformational Energy Program for Peptides

W. Wiczk · L. Łankiewicz · F. Kasprzykowski · S. Ołdziej
Z. Grzonka (✉)
Faculty of Chemistry, University of Gdańsk, Sobieskiego 18,
80-952 Gdańsk, Poland

H. Szmaciński · J. R. Lakowicz
Centre of Fluorescence Spectroscopy, School of Medicine,
Department of Biological Chemistry, University of Maryland,
108 North Greene Street, Baltimore, MD 21201-1503, USA

Introduction

Vasopressin (AVP) is an important neurohypophyseal hormone in vertebrates. It has two primary biological actions: pressor and antidiuretic. Vasopressin also exhibits typical oxytocic activities: uterine contraction and milk ejection. Arginine-vasopressin has the following structure:

$H\text{-}Cys^1\text{-}Tyr^2\text{-}Phe^3\text{-}Gln^4\text{-}Asn^5\text{-}Cys^6\text{-}Pro^7\text{-}Arg^8\text{-}Gly^9\text{-}NH_2$

The difference in the type of activity (vasopressor or oxytocic) exhibited by a particular hormone is mainly connected with the kind of amino acid occupying positions 3 and 8. On the other hand, compounds showing high selectivity or exhibiting antagonistic activity to the actions of the parent hormones are also very important from the medical perspective.

We previously reported (Grzonka et al. 1983, Gazis et al. 1984) the synthesis and interesting biological properties of arginine-vasopressin analogues containing sarcosine or N-methylalanine in position 7 and different residues in position 1. Analogues containing cysteine or β-mercaptopropionic acid (Mpa) in position 1 ([Sar^7]AVP, [Mpa^1,Sar^7]AVP, [$MeaAla^7$]AVP and [Mpa^1,$MeAla^7$]AVP) are characterized by a sharp decrease in pressor activity (100–300 times) with retained or increased antidiuretic effect ([Mpa^1,Sar^7]AVP). Furthermore, the antidiuretic/pressor activity ratio of these analogues its 35–700 times that of AVP. With the exception of [D-Arg^8]AVP analogues (Zaoral 1985) the analogues [Sar^7]AVP and [$MeAla^7$]AVP are among the most selective AVP analogues yet known.

Quite different biological profiles were observed for analogues containing deaminopenicillamine (Dmp) or β-mercapto-β,β-cyclopentamethylenepropionic acid (Cpp). These analogues ([Dmp^1,Sar^7]AVP, [Dmp^1,$MeAla^7$]AVP, [Cpp^1,Sar^7]AVP and [Cpp^1,$MeAla^7$]AVP) inhibit pressor and uterine response and have low antidiuretic activity. In the case of these inhibitory analogues the "additivity" or "non-additivity" of substitution, which can be used to explain the changes of the activity of the [Mpa^1, $MeAla(Sar)^7$]AVP analogues, seems to fail. This is prob-

ably due to the greater importance of position 1 for antagonistic potencies of the AVP analogues.

Here we report fluorescence studies of these interesting analogues. Using the frequency-domain technique we measured fluorescence decay times of the tyrosyl residue for each analogue. Based on the Förster energy transfer theory using [Asu^{1,6}]AVP (an analogue of AVP in which the disulphide bridge -S-S- is substituted by the -CH_2-CH_2-group) as a donor we calculated the distance and distance distribution between the tyrosyl residues and the disulphide bridge. We compared the results obtained with Monte Carlo simulation results (ECEPP/3 force-field).

Materials and methods

Synthesis

Analogues of arginine-vasopressin, except [Asu^{1,6}]AVP which was purchased from Aldrich and used in experiments without purification, were obtained by the solid-phase method. The α-amino groups of amino acids were protected by the *t*-butyloxycarbonyl group. The side chains of cysteine and tyrosine, and the mercapto group of β-mercaptopropionic acid, deaminopenicillamine and β-mercapto-β,β-cyclopentamethylenepropionic acid were protected by the benzyl group. The quanidino group of arginine was protected by the tosyl group. *N-t*-butyloxycarbonyl-glycine was attached to the chloromethylated polystyrene resin (Bio-Rad, 1.37 mequiv./g) by the method described by Gisin et al. (1973). After eight cycles of synthesis, the peptide was cleaved from the resin by ammonolysis. The protecting groups were removed by reduction with sodium in liquid ammonia. The disulphide bridge was formed by oxidation with iodine in diluted methanolic solution acidified with acetic acid. The crude peptide was purified by RP-HPLC on the Vydac C-18 column, then by ion-exchange chromatography (S-Sepharose FF) and finally desalted on Sephadex G-15. The overall yields of pure peptides were 15–20%. Each compound displayed the correct molecular ion peak by FDMS and gave the correct amino acid composition.

Fluorescence measurements

Frequency-domain data were obtained on an instrument with a frequency limit of 2 GHz (Lakowicz et al. 1986). The excitation source was the 3.795 MHz cavity damped output from a Coherent Model 700 dye laser with the dye Rhodamine 6G. The dye laser was synchronously pumped at 75.9 MHz using a mode-locked argon ion laser, Coherent Innowa 15, about 900 mW at 514 nm. The visible cavity-damped output of the dye laser was typically near 80 mW. To obtain 287 nm excitation of tyrosine we used a Spectra Physics Model 390 frequency doubler, with a KDP crystal. The detector was a microchannel plate photomultiplier, Hamamatsu R1564U.

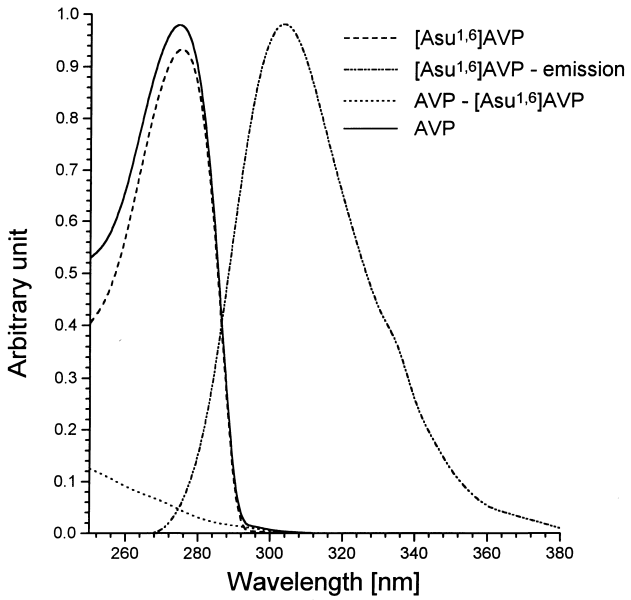

Fig. 1 Absorption spectra of [Arg^8]-vasopressin (*solid line*), [Asu^{1,6}]AVP (*dashed line*) and difference between absorption spectra of AVP and its [Asu^{1,6}] analogue (*dotted line*). *Dot-dash line* represents emission spectrum of [Asu^{1,6}]AVP

The experiments were performed in 10 mM MOPS buffer (pH = 7.0) at 20 °C. The emission was observed through an interference filter with a maximum of transmittance at 302 nm (10 nm bandpass). A magic-angle polarization was used.

For least squares analysis the uncertainties were taken as $\delta\phi = 0.3°$ and $\delta m = 0.006$. The steady-state fluorescence spectra were obtained on an LSM 8000 fluorimeter with 4 nm bandwidth for excitation and 8 nm for emission, excitation wavelength 287 nm. The quantum yields were measured relative to a value of 0.14 for tyrosine in water at 20 °C (Chen, 1967).

The value of the Förster critical distance (R_0) was calculated using emission spectra and the quantum yield of the [Asu^{1,6}]AVP analogue, and the difference between the absorption spectra of AVP and [Asu^{1,6}]AVP ($R_0 = 8.8$ Å, Fig. 1) (Szmaciński et al. 1991, 1996).

Monte Carlo simulations

The conformational space of arginine-vasopressin analogues was explored using the Electrostatically-Driven Monte Carlo (EDMC) method (Ripoll and Scheraga 1988; Vila et al. 1991; Williams et al. 1992; Li and Scheraga 1987, 1988). Briefly, this method is based on perturbing an arbitrary starting energy-minimized conformation, subsequent energy minimization of the perturbed conformation, and comparison of the resulting energy with the energy of the starting conformation. Some of the perturbations are directed at the optimization of the electrostatic interactions within the polypeptide chain. If the energy of

the new conformation appears lower, the new conformation is accepted; otherwise the Metropolis test is performed to accept or reject the new conformation. The new conformation replaces the starting one, if accepted, and the procedure is repeated. The process is iterated until either no new conformation can be found or a sufficient number of conformations have been accepted.

Conformational energy was evaluated using the ECEPP/3 (Empirical Conformational Energy Program for Peptides) force field (Némethy et al. 1992) The atomic charges and valance geometry for the Cpp, Mpa and Dmp molecules were taken from previous calculations (Liwo et al. 1988, Tarnowska et al. 1993a). The geometry of the *N*-methylated groups of Sar and MeAla was modified according to the work of Manavalan and Momany (1980). In order to simulate the experimental conditions, in one series of simulations we considered hydration contributions to energy by using a model with a 1.4 Å radius solvent sphere with atomic solvation parameters optimized using nonpeptide data (SRFOPT); (Vila et al. 1991, Williams et al. 1992). The set of initial conformations of vasopressin analogues for EDMC runs was taken from previous calculations (Liwo et al. 1988; Shenderovich et al. 1991; Tarnowska et al. 1993a).

Each of the EDMC runs was terminated after 50 energy-minimized conformations were accepted. The parameters controlling the EDMC runs were as follows: temperature = 1000 K; maximum number of allowed repetitions of the same minima = 50; maximum number of rejected conformations until the backtrack-type motion is attempted = 100. A total of 300 conformations were obtained in each series of simulations for each analogue.

In order to group the conformations obtained into families of similar conformations, the minimal-tree algorithm of cluster analysis was employed (Spätz 1980). The root mean square (RMS) deviation between the backbone heavy atoms at an optimum superposition was taken as the measure of the difference between two conformations. The RMS cut-off was 1.0 Å, the distance between the Tyr^2 and S-S chromophores was calculated as the distance between the geometric centers of the tyrosine ring and the point between the cystine sulphurs.

Using the ECEEP/3 force field which assumes rigid valance geometry requires less computational time than using a force field with flexible valance geometry, because of the smaller number of variables and the smaller number of terms in the expression for conformational energy. The conformational search can therefore be more extensive with rigid valance geometry. Moreover, it has been shown that the agreement between theoretically calculated properties of a model system and the corresponding experimental values is even better in the case of the ECEPP/2 force field (the predecessor of ECEPP/3) than for the force field that uses flexible valance geometry (Roterman et al. 1989a, b). The SRFOPT solvation model employed together with the ECEPP/3 force field enables conformational calculations in the presence of water, i.e. under the conditions of the experimental work in this report. The EDMC method used in this study has been shown to be a very powerful technique for a conformational search; it has also been shown to be able to locate the global minimum of Met-enkephalin (Ripoll and Scheraga 1988) and mellittin (Ripoll and Scheraga 1988). The EDMC method used together with the ECEPP/3 + solvation force field has been shown to be able to locate the native structures of bovine pancreatic trypsin inhibitor (Vila et al. 1992) and avian pancreatic polypeptide (Liwo et al. 1993) as the lowest-energy conformations compared to the non-native structures.

Theory and calculations

Multiexponential decays

Fluorescence intensity decays can be described as the sum of exponentials

$$I(t) = I_0 \sum_i \alpha_i \exp(-t/\tau_i) \tag{1}$$

where the τ_i are the individual decay times and α_i the associated pre-exponential factors. The fractional contribution of the *i*-th component to the total fluorescence is

$$f_i = \frac{\alpha_i \tau_i}{\sum_j \alpha_j \tau_j} \tag{2}$$

where $\sum_i f_i = 1$. Since the frequency-domain data are collected without regard for the total intensity, it is also customary to normalize the α_i values, i.e. $\sum_i \alpha_i = 1$. Mean lifetime values were calculated according to

$$\langle \tau \rangle = \sum_i f_i \tau_i \tag{3}$$

Fluorescence quenching

Consider a fluorophore which displays a single-exponential decay. Following δ-function excitation the time dependend intensity is

$$I(t) = I_0 \exp(-t/\tau_0) \tag{4}$$

where τ_0 is the decay time in the absence of quenching. Suppose the fluorophore is in homogenous solution and surrounded by randomly distributed quenchers. Predictions of the intensity decays for such samples have been the subject of several significant publications (Lakowicz et al. 1987b, and reference therein).

The quenching rate constant $k(t)$ is complex and depends upon the assumptions used in its derivation. The simplest case is obtained by assuming the concentration gradient around the fluorophore is a step function with an increase from 0 to the bulk concentration [*Q*] at the interaction radius *R*. This radius is taken as the sum of the radii of the fluorophore and the quencher. This assumption means the fluorophore is quenched instantaneously when the quencher diffuses to the boundary at $r = R$. Then, ac-

cording to the Smoluchowski-Einstein diffusion theory, the time-dependent rate constant is given by

$$k(t) = 4\pi DN' R\left(1 + \frac{R}{(\pi Dt^{1/2})}\right) \tag{5}$$

where N' is $6.02 \cdot 10^{20}$ and D is the sum of the diffusion coefficients. Evidently, the transient effect will be the largest for small values of t and slow diffusion.

If the quenching rate constant becomes diffusion controlled and independent of time, the intensity decay is single exponential

$$I(t) = I_0 \exp\left(\frac{t}{\tau_i} - k[Q]t\right) \tag{6}$$

$$k = 4\pi N' DR \tag{7}$$

Equations (6) and (7) are the usual expressions for analysis of quenching data without consideration of transient effects and lead to the Stern-Volmer equation. For purely collisional quenching the decay time is

$$\tau^{-1} = \tau_0^{-1} + k[Q] \tag{8}$$

which on rearrangement yields

$$\frac{\tau_0}{\tau} = 1 + k\tau_0[Q] = \frac{F_0}{F} \tag{9}$$

For collisional quenching the intensities (F_0 and F) are proportional to the decay times, so F_0/F is expected to be equivalent to τ_0/τ.

Fluorescence resonance energy transfer

If a D-A (donor-acceptor) pair is connected by a flexible linker, then one can expect a range of D-A distances. We have analyzed the heterogenous energy transfer in terms of distance distribution functions for the distance between the donor (e.g. a point in the center of the phenol ring) and the acceptor (e.g. a point in the center of the disulphide bond (Lakowicz et al. 1991)). In this case the intensity decay is given by

$$I_{DA}(t) = \int_{r_{\min}}^{r_{\max}} P(r) \sum \alpha_{D_i} \exp\left[-\frac{t}{\tau_{D_i}} - \frac{t}{\tau_{D_i}}\left(\frac{R_0}{r}\right)^6\right] \mathrm{d}r \tag{10}$$

where α_{D_i} and τ_{D_i} are the intensity decay parameters in the absence of energy transfer. These parameters are recovered from the measurements in the absence of an acceptor and are held constant during the distance distribution analysis. In the present paper the values of α_{D_i} and τ_{D_i} are obtained from a multi-exponential analysis of the tyrosyl fluorescence decay of the Asu-analogue.

R_0 is the Förster critical distance which can be calculated from spectral properties of the chromophores:

$$R_0^6 = \frac{9000 \ln(10)\kappa^2 \phi_D^0}{128\pi^5 N n^4} \int F_D(\lambda)\varepsilon_A(\lambda)\lambda^4 \mathrm{d}\lambda \tag{11}$$

where:

- n is the refractive index,
- N is the Avogadro number,
- ϕ_D^0 is the donor fluorescence quantum yield in the absence of an acceptor,
- $F_D(\lambda)$ is the emission spectrum of the donor, the area being normalized to unity,
- $\varepsilon_D(\lambda)$ is the excitation coefficient (in M^{-1} cm^{-1}) of the acceptor at the wavelength λ (in nm),
- κ^2 is the orientation factor.

The calculation of distances also requires knowledge of κ^2. In our paper we assume $\kappa^2 = 2/3$ as in the work by Szmaciński et al. (1996). Such an assumption is plausible because of the short correlation time (37 ps) corresponding to the rotation of the phenolic chromophore of tyrosine in vasopressin (Gryczynski et al. 1991), which should lead to averaging of the orientation factor. There are also previously published data about the relation between κ^2 and parameters of distance distribution showing that the parameters calculated for $\kappa^2 = 0.6$ and for $\kappa^2 = 2$ differ at most by several percent (Eis and Millar 1993; Wu and Brand 1992) which is, in our case, within the range of experimental error.

The fitting function we used for the distance distribution is a truncated Gaussian function i.e.

$$\begin{cases} P(r) = \dfrac{1}{Z}\exp\left[-\dfrac{1}{2}\left(\dfrac{r - R_{av}}{\sigma}\right)^2\right] & \text{for } r_{\min} < r < r_{\max} \\ P(r) = 0 & \text{elsewhere} \end{cases} \tag{12}$$

where the normalization factor is

$$Z = \int_{r_{\min}}^{r_{\max}} \exp\left[-\frac{1}{2}\left(\frac{r - R_{av}}{\sigma}\right)^2\right] \quad \text{for } r_{\min} < r < r_{\max} \tag{13}$$

The average distance and standard deviation of untruncated Gaussian function are R_{av} and σ, respectively. The width of the distributions are reported in terms of the half-width (full-width at half-maximum probability, *hw*). For a Gaussian, $hw = 2.3548\ \sigma$. The Förster resonance energy transfer occurs on the nanosecond time scale and it does not require diffusive motion to occur. The extent of energy transfer can be affected by the rate of the diffusion, such effects are expected to be modest within the time scale of tyrosyl fluorescence decay (Szmaciński et al. 1996). In the present paper we neglected the influence of diffusion on the distance distribution of vasopressin analogues.

Irrespective of the model assumed for the intensity decay, the frequency-domain data can be calculated from the sine and cosine transform of $I(t)$

$$N_\omega = \frac{\int I(t)\sin(\omega t)\mathrm{d}t}{\int I(t)\mathrm{d}t} \tag{14}$$

$$D_\omega = \frac{\int I(t)\cos(\omega t)\mathrm{d}t}{\int I(t)\mathrm{d}t} \tag{15}$$

where ω is the circular modulation frequency ($2\pi \cdot$ frequency, in hertz). The calculated (c) values of the phase

angle ($\phi_{c\omega}$) and the demodulation ($m_{c\omega}$) are given by

$$\tan \phi_{c\omega} = \frac{N_\omega}{D_\omega} \tag{16}$$

$$m_{c\omega} = \left(N_\omega^2 + D_\omega^2\right)^{1/2} \tag{17}$$

The parameters (α_i, τ_i, hw and R_{av}) are varied to yield the best fit between data and the calculated values, as indicated by a minimum values for the goodness of fit parameter χ_R^2.

$$\chi_R^2 = v^{-1}\left[\sum\left[\frac{\left(\phi_\omega - \phi_{c\omega}\right)^2}{\delta\phi^2}\right] + \left[\frac{\left(m_\omega - m_{c\omega}\right)^2}{\delta m^2}\right]\right] \tag{18}$$

where v is the number of degrees of freedom and $\delta\phi$ and δm are the uncertainty in the phase and modulation values, respectively.

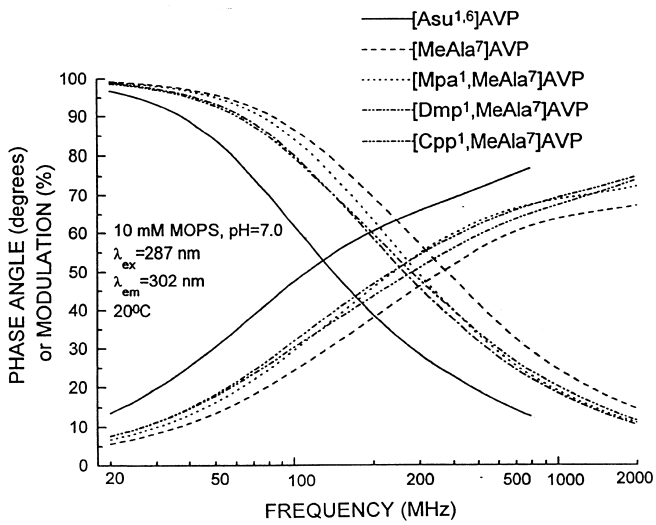

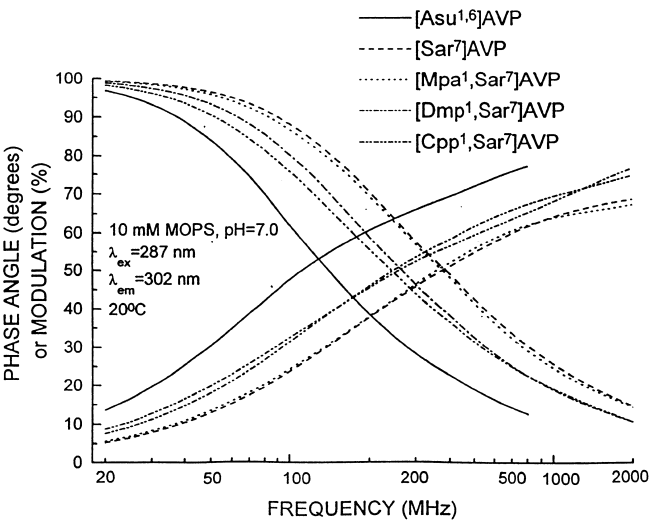

Fig. 2 Frequency-domain intensity decays for [Asu^{1,6}]AVP and [MeAla^7]AVP analogues (*top*) and [Sar^7]AVP analogues (*bottom*) in 10 mM MOPS buffer. Because of a large number of measurement points and curves, for the sake of clarity, no experimental points were marked on the curves in the figures. The quality of fitting of the calculated curves to the experimental point, expressed as the χ_R^2 values, is presented in Table 1

Results

Lifetime analysis

Frequency-domain data for vasopressin analogues are shown in Fig. 2. It was necessary to use modulation frequencies as high as 2 GHz to observe the complete frequency response of the emission.

The fit to a single-exponential decay is obviously not able to account for the data. The double-exponential model is also inadequate, as can be seen from the relative χ_R^2 values (Table 1). Three decay times were needed to account for the data, resulting in a four to five-fold decrease in χ_R^2 as compared to the double-exponential fit.

Substitution of Pro^7 in arginine-vasopressin by either sarcosine or N-methylalanine changed only slightly the mean fluorescence lifetime of tyrosyl residue: $\tau = 0.75$ ns for [Sar^7]AVP, $\tau = 0.79$ ns for [MeAla^7]AVP (this work), and $\tau = 0.85$ ns for AVP (Szmaciński et al. 1991, Szmaciński et al. 1996). In contrast we have observed that substitution at position 1 has a larger influence on the tyrosyl mean fluorescence lifetime. Peptides containing cysteine in position 1 had the shortest fluorescence lifetime. Modification of the cysteine residue (deamination or alkylation of β-carbon) resulted in a longer lifetime. The longest mean fluorescence lifetime ($\tau = 1.24$ ns) was observed for [Cpp^1,Sar^7]AVP. It is possible that the decay times have their origin in a distinct conformational state, i.e. the rotamer model, as described by Ross et al. (1986, 1992) for oxytocin, tyrosine analogues (Laws et al. 1986), and for tryptophan (Tilstra et al. 1990).

All analogues which contain the disulphide-bridge have shorter fluorescence lifetimes than the [Asu^{1,6}]AVP analogue, in which the disulphide-bridge is substituted by the -CH_2-CH_2-group. The large difference in the mean lifetimes between [Asu^{1,6}]AVP and other AVP analogues suggests additional mechanisms of fluorescence quenching caused by the presence of the disulphide bridge. There have been three different models proposed for quenching: static (Ross et al. 1986), dynamic and static (Swadesh and Scheraga, 1987) and diminished fluorescence due to vibrational dissipation of energy (Cowgill 1967). Moreover, Shafferman and Stein (1974), and Szmaciński et al. (1991, 1995) have proposed the additional mechanism of quenching by Förster-type energy transfer from tyrosine (donor) to disulphide bridge (acceptor), which we have used in this work.

Table 1 Tyrosyl fluorescence intensity in 10 mM MOPS buffer pH=7.0, at 20 °C, λ_{ex}=287 nm, λ_{em}=302 nm

Compound	τ_i [ns]	α_i	f_i	$\langle\tau\rangle$ [ns]	χ^2_R
[Sar^7]AVP	0.57	1.00	1.00	–	263.0
	0.15	0.519	0.161		
	0.86	0.481	0.838	0.72	6.7
	0.04	0.396	0.037		
	0.32	0.334	0.282		
	0.96	0.271	0.681	0.75	1.5
[Mpa^1,Sar^7]AVP	0.83	1.00	1.00	–	204.0
	0.18	0.420	0.107		
	1.11	0.580	0.893	1.01	3.8
	0.03	0.432	0.021		
	0.36	0.224	0.162		
	1.19	0.345	0.817	1.03	1.5
[Dmp^1,Sar^7]AVP	0.82	1.00	1.00	–	253.6
	0.22	0.496	0.151		
	1.18	0.504	0.849	1.04	5.5
	0.08	0.297	0.038		
	0.45	0.357	0.247		
	1.34	0.345	0.715	1.07	1.7
[Cpp^1,Sar^7]AVP	0.91	1.00	1.00	–	326.9
	0.28	0.621	0.239		
	1.47	0.379	0.761	1.19	4.8
	0.17	0.444	0.109		
	0.72	0.361	0.347		
	1.84	0.195	0.517	1.22	1.0
[MeAla^7]AVP	0.57	1.00	1.00	–	312.8
	0.14	0.538	0.160		
	0.85	0.463	0.840	0.73	9.9
	0.05	0.451	0.061		
	0.46	0.381	0.441		
	1.17	0.168	0.498	0.79	1.7
[Mpa^1,MeAla^7]AVP	0.79	1.00	1.00	–	201.4
	0.12	0.397	0.074		
	0.98	0.603	0.926	0.92	3.0
	0.07	0.378	0.045		
	0.56	0.231	0.218		
	1.11	0.392	0.737	0.93	1.6
[Dmp^1,MeAla^7]AVP	0.75	1.00	1.00	–	393.4
	0.20	0.515	0.158		
	1.10	0.485	0.842	0.96	6.9
	0.09	0.323	0.047		
	0.46	0.318	0.297		
	1.31	0.396	0.656	1.00	1.10
[Cpp^1,MeAla^7]AVP	0.77	1.00	1.00	–	318.9
	0.22	0.568	0.195		
	1.21	0.432	0.805	1.02	7.7
	0.10	0.347	0.059		
	0.52	0.413	0.352		
	1.50	0.240	0.589	1.07	1.3

Distance distribution analysis

The intensity decays of vasopressin analogues could be analyzed in several ways, including multiexponential (Table 1 and Fig. 2) (Lakowicz 1983), and lifetime distribution models (Alcala et al. 1987; Lakowicz et al. 1987a). However, parameters obtained in these models do not reflect the molecular feature of the distance distribution between the tyrosine and disulphide bridge. Hence the intensity decays were analyzed in a pairwise manner (donor vs donor-acceptor pair) to recover the mean (R_{av}) and half-

Table 2 Recovered distance distributions and energy transfer parameters for the series of the AVP analogues

Analogue	R_{av} [Å]	hw [Å]	χ^2_R	E_T^b	E_T^c
[Sar^7]AVP	7.57[a]	2.67[a]	3.2	0.70	0.69
[Mpa^1,Sar^7]AVP	8.76	2.46	3.4	0.52	0.53
[Dmp^1,Sar^7]AVP	8.55	3.50	2.2	0.55	0.55
[Cpp^1,Sar^7]AVP	7.68	6.83	2.1	0.63	0.61
[MeAla^7]AVP	7.46	3.12	3.6	0.71	0.72
[Mpa^1,MeAla^7]AVP	8.57	1.61	3.7	0.55	0.58
[Dmp^1,MeAla^7]AVP	8.21	3.60	1.8	0.60	0.61
[Cpp^1,MeAla^7]AVP	8.10	4.36	1.9	0.61	0.59

[a] Using differential absorption spectra of AVP and [Asu^{1,6}]AVP analogue (R_0=8.78 Å)

[b] Calculated from equation: $E_T = \int P(r)\,\frac{P_0^6}{P_0^6 + r^6}\,dr$

[c] Calculated from steady-state $E_T = 1 - Q_{DA}/Q_D$

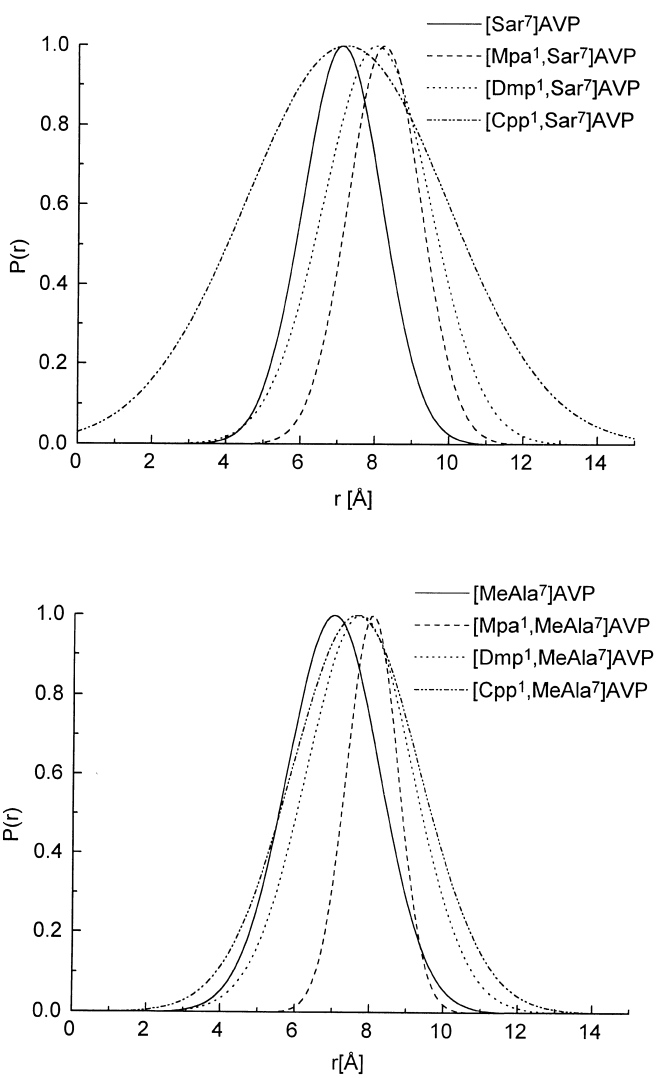

Fig. 3 Tyrosine-to-disulfide bridge distance distributions for [Sar^7]AVP analogues (*top*) and [MeAla^7]AVP analogues (*bottom*) in 10 mM MOPS (pH = 7.0) at 20 °C

width (*hw*) of the distance distribution. In this analysis the parameters describing the intensity decay of the donor (α_i and τ_i in Table 1) are held constant in the fitting procedure. Assuming that the energy transfer is Förster-type we have obtained distance distribution parameters using a truncated Gaussian as the distance distribution function (Lakowicz et al. 1991). The results of analysis of distance distribution are summarized in Table 2. Plots of recovered distance distribution for all analogues of vasopressin are in Fig. 3.

As can be seen in Table 2 and Fig. 3 the average distances for all analogues are between 7 and 8 Å and half-width (*hw*) between 2.5 and 4 Å (using R_0 calculated for cystine). Analogues containing cysteine have the smallest R_{av} values. Analogues with modifications in position 1 (Mpa, Dmp, Cpp) have higher R_{av} values, but there is no correlation between R_{av} values and dimensions of alkyl substituents on the β-carbon in the residue in position 1. We have found (for both groups of analogues) a correlation between the size of substituents and the half-width of distribution (*hw*). We have observed an increase of half-width of the distributions with the size of the alkyl substituents. Surprisingly we have also discovered a relatively wide distribution for [Cpp^1,Sar^7]AVP, which was 50% wider than for the appropriate analogue with *N*-methyl-alanine in position 7. The recovered distance distribution parameters for [Sar^7]AVP and [MeAla^7]AVP are similar to those for AVP (R_{av} = 7.51 Å, *hw* = 2.63 Å) published by Szmaciński et al. (1991, 1995). This suggests a small influence of position 7 on conformational features of the vasopressin ring.

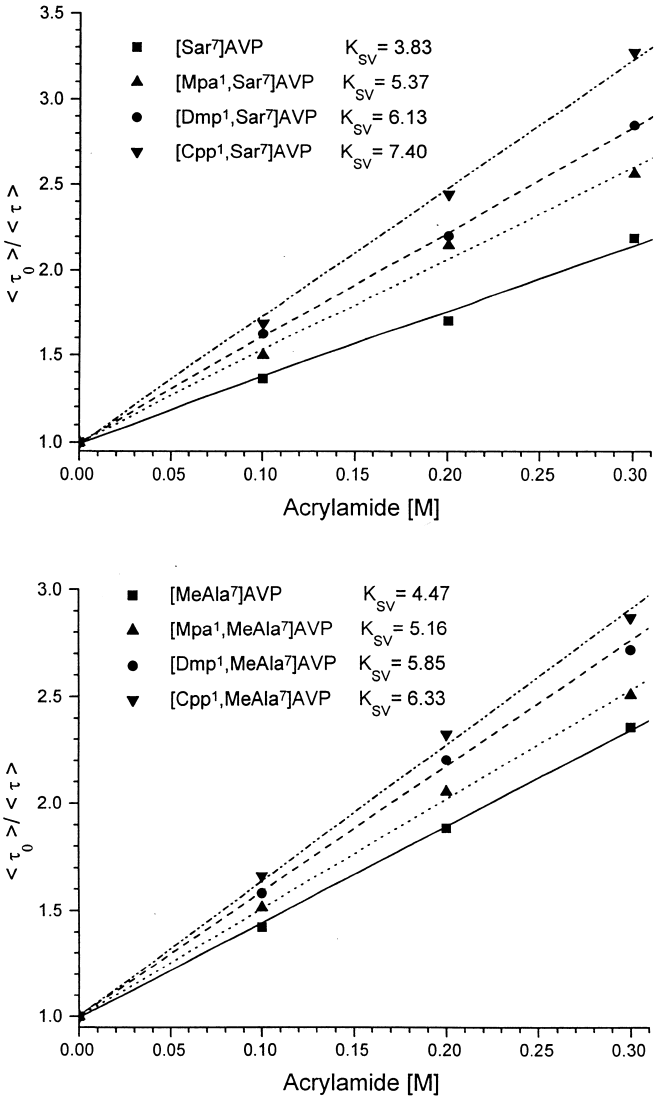

Fig. 4 Stern-Volmer plots for [Sar^7]AVP and [MeAla^7]AVP analogues obtained based on average decay times for non-quenched and quenched samples by acrylamide

Fluorescence quenching

We used collisional quenching to estimate exposure of the tyrosyl residue to solvent. Acrylamide is know to be a quencher of protein fluorescence, especially for tryptophan-containing proteins (Eftink and Ghiron 1981), it is also an effective quencher for tyrosine fluorescence (Lakowicz 1983; Follenius and Gerard 1983). The Förster critical distance (R_0) for acrylamide (acceptor) and tyrosine (donor) is 3.6 Å (Micewicz et al. 1995). Hence, the quenching of tyrosine due to energy transfer is negligible, and in any event, molecular contact seems to be required for quenching. However the mechanism of fluorescence quenching still remains unknown.

The frequency-domain data were analyzed by using the decay law expected from the Smoluchowski theory of quenching. The parameters recovered from multiexponential analysis of quenched samples are shown in Table 3. It is known that, with quenching, homogenous decays generally became more heterogenous. However, the intensity decays of vasopressin analogues are already strongly heterogenous, and the effect of quenching was not evident as a further increase in χ^2_R (Table 3).

We used the mean decay times shown in Table 3 to construct Stern-Volmer plots (Fig. 4). In both groups of analogues, the Stern-Volmer constant increases with the size of the alkyl substituent on the β-carbon. Because of the same tendency of increasing mean lifetime with the size of the alkyl substituents of non-quenched derivatives ([Sar^7]AVP, [MeAla^7]AVP), rate constants for fluorescence quenching are increasing in both groups of analogues but the increase is not so significant. They are in the range $5-6 \cdot 10^9$ M^{-1} s^{-1} for both groups of analogues (sarcosine or *N*-methylalanine in position 7). The larger alkyl substituents (Dmp, Cpp) cause little increase in the quenching rate constants in comparison with parent compounds and desamino analogues. The substitution in position 7 only change the quenching rate constants for analogues with a small substituent in position 1. Based on the frequency-domain data obtained for quenched and non-quenched samples we calculated diffusion coefficients using Smoluchowski's model. The results of the global analysis (acrylamide concentration 0–0.3 M) are summarized in

Table 3 Multiexponential analysis of tyrosyl fluorescence quenched by acrylamide in 10 mM MOPS buffer pH = 7.0, at 20 °C, λ_{ex} = 287 nm, λ_{em} = 302 nm

Acrylamide	τ_i [ns]	α_i	f_i	$\langle\tau\rangle$ [ns]	χ^2_R		
					1 exp[a]	2 exp[b]	3 exp[c]
			[Sar^7]AVP				
	0.02	0.575	0.053				
0.1	0.33	0.296	0.456	0.55			
	0.82	0.129	0.491		408.1	17.1	1.1
	0.02	0.619	0.076				
0.2	0.31	0.293	0.546	0.44			
	0.71	0.088	0.378		558.4	14.1	1.9
	0.02	0.699	0.094				
0.3	0.25	0.209	0.436	0.34			
	0.53	0.092	0.436		908.7	12.9	2.5
			[Mpa^1,Sar^7]AVP				
	0.03	0.513	0.042				
0.1	0.35	0.219	0.243	0.69			
	0.84	0.268	0.715		361.1	8.2	1.3
	0.02	0.556	0.059				
0.2	0.32	0.358	0.614	0.48			
	0.86	0.068	0.327		399.2	9.2	1.3
	0.01	0.658	0.066				
0.3	0.20	0.135	0.195	0.40			
	0.49	0.207	0.739		656.8	7.6	1.3
			[Dmp^1,Sar^7]AVP				
	0.03	0.497	0.048				
0.1	0.30	0.213	0.210	0.66			
	0.80	0.290	0.742		446.6	11.9	2.2
	0.02	0.579	0.064				
0.2	0.28	0.208	0.276	0.49			
	0.65	0.213	0.660		494.2	10.8	2.4
	0.01	0.716	0.064				
0.3	0.19	0.133	0.233	0.38			
	0.51	0.151	0.704		574.6	9.6	1.8
			[Cpp^1,Sar^7]AVP				
	0.03	0.634	0.068				
0.1	0.38	0.220	0.342	0.72			
	1.00	0.146	0.590		548.5	12.0	2.2
	0.02	0.697	0.093				
0.2	0.28	0.185	0.341	0.50			
	0.71	0.118	0.566		455.0	10.1	3.2
	0.02	0.770	0.131				
0.3	0.31	0.188	0.579	0.37			
	0.71	0.041	0.269		516.8	9.3	2.9

Acrylamide	τ_i [ns]	α_i	f_i	$\langle\tau\rangle$ [ns]	χ^2_R		
					1 exp[a]	2 exp[b]	3 exp[c]
			[MeAla^7]AVP				
	0.02	0.550	0.045				
0.1	0.34	0.331	0.503	0.55			
	0.85	0.119	0.451		346.6	17.2	1.5
	0.02	0.547	0.072				
0.2	0.28	0.306	0.488	0.42			
	0.64	0.120	0.440		459.1	10.5	1.4
	0.01	0.733	0.085				
0.3	0.17	0.132	0.262	0.34			
	0.42	0.135	0.635		669.6	8.6	1.4
			[Mpa^1,MeAla^7]AVP				
	0.02	0.495	0.040				
0.1	0.16	0.144	0.087	0.60			
	0.65	0.360	0.873		292.3	2.8	1.6
	0.02	0.597	0.054				
0.2	0.14	0.113	0.098	0.43			
	0.48	0.290	0.848		361.9	4.4	2.5
	0.01	0.733	0.078				
0.3	0.17	0.108	0.195	0.35			
	0.43	0.159	0.727		665.0	10.6	3.3
			[Dmp^1,MeAla^7]AVP				
	0.01	0.709	0.034				
0.1	0.27	0.153	0.257	0.66			
	0.83	0.138	0.709		439.7	17.8	2.3
	0.02	0.730	0.058				
0.2	0.24	0.202	0.258	0.49			
	0.62	0.212	0.648		481.9	9.3	1.8
	0.01	0.730	0.074				
0.3	0.23	0.190	0.434	0.40			
	0.61	0.080	0.492		551.4	19.8	3.6
			[Cpp^1,MeAla^7]AVP				
	0.03	0.555	0.057				
0.1	0.33	0.277	0.343	0.65			
	0.96	0.168	0.600		589.3	21.6	2.7
	0.02	0.623	0.069				
0.2	0.29	0.262	0.434	0.46			
	0.75	0.116	0.497		750.1	20.4	2.6
	0.01	0.748	0.081				
0.3	0.20	0.142	0.308	0.37			
	0.51	0.110	0.611		757.8	13.1	3.2

[a, b, c] Fit to one, two and three components. Mean lifetime $\langle\tau\rangle = f_i \tau_i$

Table 4. In all these analyses, the encounter radius was held fixed at 7 Å. The diffusion coefficients recovered for acrylamide quenching of vasopressin analogues are in the range $3-4 \cdot 10^{-6}$ cm^2/s. The relatively high χ^2 values obtained for all measurements reflect the inadequacy of the model applied (Lakowicz et al. 1987b). The results suggest that the acrylamide group can easily approach the phenolic ring of tyrosine in vasopressin analogues. The apparent diffusion coefficient reflects the degree of exposure of the tyrosyl residue to the aqueous phase, and there are no significant differences among all the analogues modified in position 1. The diffusion coefficients calculated for both groups of analogues are similar to the coefficient obtained for AVP by Gryczynski et al. (1991).

Molecular mechanics calculations

The results of molecular mechanics calculations are shown in Table 5. We can observe that the flexibility of the cyclic

Table 4 Diffusion and quenching parameters for tyrosyl fluorescence quenched by acrylamide in 10 mM MOPS buffer, pH=7.0 at 20 °C, λ_{ex}=287 nm, λ_{em}=302 nm

Compound	log D	χ^2_R	K_{SV} [M^{-1}][a]	$\langle\tau\rangle$ [ns]	$k_q \cdot 10^{-9}$ [M^{-1} s^{-1}]
[Sar^7]AVP	–5.477	2.8	3.83±0.04	0.75	5.11
[Mpa^1,Sar^7]AVP	–5.462	3.5	5.37±0.10	1.03	5.21
[Dmp^1,Sar^7]AVP	–5.408	7.0	6.13±0.13	1.07	5.73
[Cpp^1,Sar^7]AVP	–5.377	6.1	7.40±0.07	1.22	6.06
[MeAla^7]AVP	–5.488	6.5	4.47±0.09	0.79	5.58
[Mpa^1,MeAla^7]AVP	–5.487	6.9	5.16±0.09	0.93	5.48
[Dmp^1,MeAla^7]AVP	–5.414	6.8	5.85±0.07	1.00	5.85
[Cpp^1,MeAla^7]AVP	–5.388	4.7	6.33±0.09	1.07	5.92

[a] From linear fit to Stern-Volmer equation

Table 5 Conformational parameters calculated for AVP analogues. R_{cal} – distance between chromophores calculated for the lowest energy conformation, Range – the range of distances between chromophores calculated for all generated conformations. Conformational code for the lowest energy conformation (Zimmermann et al. 1977)

Analogues	R_{cal} [Å]	Range [Å]	Conformational code
[Sar^7]AVP	7.2	6.9–8.9	GGDBDCF
[Mpa^1,Sar^7]AVP	8.1	7.5–9.0	BFACDDA
[Dmp^1,Sar^7]AVP	8.0	6.5–9.3	CBGEDCA
[Cpp^1,Sar^7]AVP	7.8	6.4–9.3	GFACDAE
[MeAla^7]AVP	7.3	7.0–9.0	AFACDDA
[Mpa^1,MeAla^7]AVP	8.2	7.5–9.0	EDGDDC*A
[Dmp^1,MeAla^7]AVP	8.2	6.5–9.3	AAGDDDA
[Cpp^1,MeAla^7]AVP	7.7	6.5–9.2	EAADDDA

part of the peptide is higher for analogues with Cys of Mpa in position 1. (By 'flexibility' we mean the conformational space accessible to a molecule or its part; it has no relation to physical motion of molecule). Analogues with Dmp or Cpp residue in position 1 have a more rigid conformation. Acyclic tripeptide and amino acid residues in position 7 have only a small influence on the conformation of cyclic part of peptide, which is in a good agreement with previous calculations (Liwo et al. 1988; Shenderovich et al. 1991; Tarnowska et al. 1993b). Calculated distances between the -S-S- bridge and the phenol ring show higher mobility of the tyrosyl residue in analogues with Dmp or Cpp in position 1 (distance from 6.5 to 9.3 Å and from 6.3 to 9.2 Å, respectively) than in compounds with Cys or Mpa residues in position 1 (distance from 7.4 to 9.0 Å).

Discussion

We have investigated fluorescence spectral properties and theoretical conformations for a series of AVP analogues containing sarcosine or *N*-methylalanine in position 7 and a different residue in position 1 (Cys, Mpa, Dmp, Cpp). We observed changes in mean fluorescence lifetimes of the tyrosyl residue for the groups of analogues having different residues in position 1. These changes appear to have their origin in the distance distribution changes between acceptor (disulphide bridge) and donor (tyrosine) observed using time-resolved studies of energy-transfer.

The parameters of the distance distributions were obtained by fitting Eq. (10) to the experimental intensity-decay data by assuming the Förster mechanism of energy transfer. One rationale for this assumption was based on the results of earlier studies of Szmaciński et al. (1996) on the fluorescence-energy transfer of oxytocin and [Arg^8]-vasopressin in various solvents and at temperatures, using steady-state and time-resolved fluorescence spectroscopy. By analysing the dependence of the fluorescence quantum yield and decay time on solvent viscosity the authors excluded the contribution of the alternative Dexter mechanism. The other reason for assuming the Förster mechanism is that in extensive conformational studies of vasopressin and its analogues carried out with the use of powerful Monte Carlo and molecular dynamics conformational-search protocols with force fields that included hydration (Liwo et al. 1988, 1996; Shenderovich et al. 1991; Tarnowska et al. 1993), the phenol ring of Tyr^2 and the disulfide bridge are far apart in all of the low-energy conformations, whereas the efficiency of energy transfer through the Dexter mechanism decays very fast (exponentially) with the distance. In practical terms, for the energy transfer to occur contact approach of the two chromophores is required. Analogues containing cysteine in position 1 had the smallest mean distance between chromophores. Other analogues had only slightly larger mean distances and the difference was about 0.5 Å. These results are in good agreement with theoretical data obtained by molecular mechanics calculations (Tables 2 and 5).

Interestingly, we found a direct correlation between dimensions of the substituent on the α or β-carbon of the residue in position 1 and the half-width (*hw*) of the distance distribution. The half-widths increased with the dimensions of alkyl(amino) substituent. Theoretical calculations showed a similar correlation, but the obtained distance distribution parameters had a smaller range (Tables 2 and 5). Some differences between the calculated and measured half-width of the distance distributions can occur because of the approximations inherent in the calculations, mainly the assumption of a Gaussian shape for the distance distribution. This model is an approximation, especially for molecules containing only few amino acid residues (Leclerc et al. 1977, 1978). On the other hand, because the rotation of the phenolic ring of tyrosine about the χ^2 angle is fast, the above-mentioned assumption that κ^2 is constant should not, to our knowledge, influence the distance distribution beyond the range of the experimental error.

Analogues having larger half-width of distance distribution (Cpp or Dmp in position 1) have exhibited antagonistic activity (Gazis et al. 1984). On the other hand the agonistic analogues of AVP (Mpa or Cys in position 1) were characterized by smaller half-width of the distance distribution. This suggests higher lability of the cyclic part in the analogues with Cpp or Dmp than those with Mpa or Cys. Theoretical calculations and NMR data (Shendero-

vich et al. 1991) have shown quite a different pattern: analogues with Cpp or Dmp have a more rigid conformation for the a cyclic part of the peptide. This suggests that Cpp and Dmp substitutions in position 1 have caused more rigid conformation of the cyclic peptide ring and at the same time higher mobility of the phenol ring of tyrosine. Measurements of tyrosine fluorescence quenching showed no shielding effect of tyrosine by the residue in position 1, even by a bulky alkyl group such as cyclohexyl (Cpp substitution). Diffusion constants were similar for all analogues which is in a good agreement with the previous statement about mobility of the phenol ring of tyrosine in Cpp and Dmp modified analogues.

The QSAR studies (Tarnowska et al. 1992) revealed the importance of positions 1 and 2 for the antagonistic activity of AVP analogues. Our experiments have shown that bulky substituents in position 1, making the conformation of the cyclic part of the analogues more rigid, resulted in higher mobility of the phenol ring of tyrosine, which can be important for the antagonists of AVP.

The fluorescence studies and theoretical calculations showed no direct influence of substitution in position 7 on the conformation of the cyclic part of analogues. The changes in the mean life-time of the pairs of analogues with sarcosine or *N*-methylalanine in position 7 were not significant (Table 1). At the same time we did not observe a clear correlation between the other fluorescence parameters (distance distribution, quenching) and the type of substitution at position 7. However from the biological point of view, position 7 in the AVP analogues is very important, particularly for the selectivity of action (Grzonka et al. 1983). To estimate an interaction between the cyclic and the acyclic part of analogues we have started conformational studies using analogues modified in position 9.

Acknowledgments This work was supported by Stiftung für deutsch-polnische Zusammenarbeit (1384/94/IS) (Z.G.) and grants from the National Institute of Health (GM 35154 and GM 39617) and with support for the Centre of Fluorescence Spectroscopy from the National Science Foundation (DIR-8710401) and the National Institute of Health (RR-08119 and RR-07510) (J.R.L.).

References

Alcala JR, Gratton E, Prendergast FG (1987) Resolvability of fluorescence lifetime distributions using phase fluorymetry. Biophys J 51:587–596

Chen RF (1967) Fluorescence quantum yields of tryptophan and tyrosine. Anal Lett 1:35–42

Cowgill RW (1967) Fluorescence and protein structure XI. Fluorescence quenching by disulphide and sulfhydryl groups. Biochem Biophys Acta 140:37–44

Eftink MR, Ghiron CA (1981) Fluorescence quenching studies with proteins. Anal Biochem 114:199–227

Eis PS, Millar D (1993) Conformational distribution of four-way junction revealed by time-resolved fluorescence resonance energy transfer. Biochemistry 32:13852–13860

Follenius A, Gerard D (1983) Acrylamide fluorescence quenching applied to tyrosyl residues in protein. Photochem Photobiol 38: 373–376

Gazis D, Schwartz IL, Lammek B, Grzonka Z (1984) Influence of sarcosine or *N*-methylalanine in position 7 on the antagonistic properties of [1-deaminopenicillamine]- and [1-(β-mercapto-β,β-cyclopentamethylene-propionic acid)]-vasopressin. Int J Peptide Protein Res 23:78–83

Gisin BF (1973) The preparation of Merrifield-resin through total esterification with cesium salts. Helv Chim Acta 56:1476–1478

Gryczyński I, Szmaciński H, Laczko G, Wiczk W, Johnson ML, Kuśba J, Lakowicz JR (1991) Conformational differences of oxytocin and vasopressin as observed by fluorescence anisotropy decays and transient effect in collisional quenching of tyrosine fluorescence. J Fluorescence 1:163–175

Grzonka Z, Lammek B, Kasprzykowski F, Gazis D, Schwartz IL (1983) Synthesis and some pharmacological properties of oxytocin and vasopressin analogues with sarcosine and N-methyl-L-alanine in position 7. J Med Chem 26:555–559

Lakowicz JR (1983) Principles of fluorescence spectroscopy. Plenum Press, New York

Lakowicz JR, Laczko G, Gryczyński I (1986) 2 GHz frequency-domain fluorymeter. Rev Sci Instrum 57:2499–2506

Lakowicz JR, Cherek H, Gryczyński I, Joshi N, Johnson ML (1987a) Analysis of fluorescence decay kinetics measured in the frequency-domain using distributions of decay times. Biophys Chem 28:35–50

Lakowicz JR, Johnson ML, Gryczyński I, Joshi N, Laczko G (1987b) Transient effects in fluorescence quenching measured by 2-GHz frequency domain fluorymetry. J Phys Chem 91:3277–3281

Lakowicz JR, Kuśba J, Gryczyński I, Wiczk W, Szmaciński H, Johnson ML (1991) End-to-end diffusion and distance distributions of flexible donor-acceptor systems observed by intramolecular energy transfer and frequency-domain fluorimetry; resolution by global analysis of externally and non-quenched samples. J Phys Chem 95:9654–9660

Laws WR, Ross JBA, Wyssbrod HR, Beecham JM, Brand L, Sutherland JC (1986) Time-resolved fluorescence and 1H NMR studies of tyrosine analogues: correlation of NMR-determined rotamer populations and fluorescence kinetics. Biochemistry 25: 599–607

Leclerc M, Premilat S, Guillard R, Renneboog-Squilbin C, Engrelt A (1977) Interpretation of energy-transfer experiments by theoretical studies of model compounds using semiempirical potential functions. II. Monte-Carlo calculations on oligopeptides, Biopolymers 16:531–544

Leclerc M, Premilat S, Engrelt A (1978) Nonradiative energy transfer in oligopeptide chains generated by Monte-Carlo method including long-range interactions. Biopolymers 17:2459–2473

Li Z, Scheraga HA (1987) Monte Carlo-minimization approach to the multiple-minima problem in protein folding. Proc Natl Acad Sci USA 84:6611–6615

Li Z, Scheraga HA (1988) Structure and free energy of complex thermodynamic systems. J Mol Struct (Teochem) 179:333–352

Liwo A, Tempczyk A, Grzonka Z (1988) Molecular mechanics calculations on deaminooxytocin and on deamino-argine-vasopressin and on its analogues. J Comput-Aided Mol Design 2:281–309

Liwo A et al (1966) Exploration of the conformational space of oxytocin and arginine vasopressin using the electrostatically driven Monte Carlo and molecular dynamics methods. Biopolymers 38:157–175

Manavalan P, Momany FA (1980) Conformational energy studies on N-methylated analogs of thyrotropin releasing hormon, enkefalin, and luteinizing hormone-releasing hormone. Biopolymers 19: 1943–1973

Micewicz B, Liwo A, Łankiewicz L, Wiczk W (1995) Mechanism of the fluorescence quenching of tyrosine analogues by the acrylamide. Abstracts of 2nd Israeli-Polish Symposium on the Chemistry and Biology of Peptides and Proteins, Weizmann Institute of Science, Rehovot, p 38

Nemethy G, Gibson KD, Palmer KA, Yoon CN, Paterlini G, Zagari A, Rumsey S, Scheraga HA (1992) Energy parameters in polypeptide. 10. Improved geometrical parameters and nonbonded interactions for use in the ECEPP/3 algorithm with application to proline-containing peptides. J Phys Chem 96:6472–6484

Ripoll D, Scheraga HA (1988) On the multiple-minima problem in the conformational analysis of polypeptides. II. An electrostatically driven Monte Carlo method – test or poly(L-alanine). Biopolymers 27:1283–1303

Ross JBA, Laws WR, Buku A, Sutherland JC, Wyssbrod HR (1986) Time resolved fluorescence and ^{1}H NMR-determined conformations of tyrosyl residues and fluorescence decay kinetics. Biochemistry 25:607–612

Ross JBA, Wyssbrod HR, Porter RA, Schwartz GP, Michaels CA, Laws WR (1992) Correlation of tryptophan fluorescence intensity decay parameters with 1H NMR-determined rotamer conformations: [Tryptophan^2]Oxytocin. Biochemistry 31:1585–1594

Roterman IK, Gibson KD, Scheraga HA (1989) A comparison of the CHARMM, AMBER and ECEPP potentials for peptides. I. Conformational predictions for the tandemly repeated peptide(Asn-Ala-Asn-Pro)$_9$. J Biomol Struct Dynam 7:391–419

Roterman IK, Lambert MH, Gibson KD, Scheraga HA (1989) A comparison of the CHARMM, AMBER and ECEPP potentials for peptides. II. ϕ-ψ maps for N-acetyl alanine N′-methyl amide: comparisons, contrasts and simple experimental tests. J Biomol Struct Dynam 7:421–453

Shafferman A, Stein G (1974) The effect of aromatic amino acids on the photochemistry of a disulfide; energy transfer and reaction with hydrated electrons. Photochem Photobiol 20:399–406

Shenerovich MD, Kasprzykowski F, Liwo A, Sekacis I, Saulitis J, Nikiforovich GV (1991) Conformational analysis of [Cpp^1,Sar^7,Arg^8]vasopressin by ^{1}H-NMR spectroscopy and molecular mechanics calculations. Int J Peptide Protein Res 38:528–538

Späth H (1980) Cluster analysis algorithms. Halsted Press, New York, pp 170–194

Szmaciński H, Wiczk W, Fishman MN, Eis PS, Lakowicz JR (1991) Oxytocin and [Arg^8]vasopressin tyrosine-to-disulfide bridge distance distributions recovered with frequency-domain fluorescence energy transfer measurements. Biophys J 59:116a

Szmaciński H, Wiczk W, Fishman MN, Eis PS, Lakowicz JR, Johnson ML (1996) Distance distributions from the tyrosyl to disulfide residues in the oxytocin and [Arg^8]-vasopressin measured using frequency domain fluorescence resonance energy transfer. E Biophys J 24:189–193

Tarnowska M, Liwo A, Grzonka Z, Tempczyk A (1992) In: Kuchar M (ed) QSAR in design of bioactive compounds. JR Prous Science Publisher, SA, pp 361–397

Tarnowska M, Liwo A, Shenderovich MD, Lepina I, Golbraikh AA, Grzonka Z, Tempczyk A (1993a) Molecular mechanics study of the effect of substitution in position 1 on the conformational space of the oxytocin/vasopressin ring. J Comput-Aided Mol Design 7:699–720

Tarnowska M, Liwo A, Kasprzykowski F, Łankiewicz L, Grzonka Z, Ciarkowski J (1993b) Some aspects of the structure-activity relationships in oxytocin and vasopressin. Curr Topics Med Chem 1:145–154

Tilstra L, Sattler MC, Cherry WR, Barkley MD (1990) Fluorescence of a rotationally constrained tryptophan derivatives, 3-carboxy-1,2,3,4-tetrahydro-L-carboline. J Am Chem Soc 112:9176–9192

Vila J, Williams RL, Vasquez M, Scheraga HA (1991) Empirical solvation models can be used to differentiative native from near-native conformations for bovine pancreatic trypsin inhibitor. Proteins Struct Function Genet 10:199–218

Williams RL, Vila J, Perrot G, Scheraga HA (1992) Empirical solvation models in the context of conformational energy searches. Application to bovine pancreatic trypsin inhibitor. Proteins Struct Function Genet 14:110–119

Wu P, Brand L (1992) Orientation factor in steady-state and time-resolved resonance energy transfer measurements. Biochemistry 31:7939–7947

Zaoral M (1985) Vasopressin analogs with high and specific antidiuretic activity. Int J Peptide Protein Res 25:561–574

Zimmerman SS, Pottle MS, Nemethy G, Scheraga HA (1977) Conformational analysis of the twenty naturally occuring acid residues using ECEPP. Macromolecules 10:1–9